Asian Journal of Chemistry; Vol. 24, No. 7 (2012), 2891-2898

ASIAN JOURNAL OF CHEMISTRY

www.asianjournalofchemistry.co.in

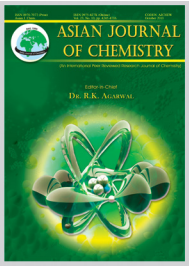

Effect of Ancillary Ligands on the Electronic Structures, DNA-binding and Spectral Properties of $[Ru(L)_2(atatp)]^{2+}$ (L = phen, bpy, dmp, tfp)

TI-FANG MIAO[1], JUN LI[2,*], YU-TING LU[3] and KANG-CHENG ZHENG[3]

[1]College of Chemistry and Materials Science, Huaibei Normal University, Huaibei 235000, P.R. China
[2]Department of Chemistry, Guangdong Institute of Education, Guangzhou 510303, P.R. China
[3]The Key Laboratory of Bioinorganic and Synthetic Chemistry of Ministry of Education, School of Chemistry and Chemical Engineering, Sun Yat-Sen University, Guangzhou 510275, P.R. China

*Corresponding authors: E-mail: lijun61@hotmail.com

(*Received*: 18 June 2011; *Accepted*: 1 February 2012) AJC-11028

The effect of ancillary ligands on the electronic structures and DNA-binding properties of Ru(II) polypyridyl complexes $[Ru(L)_2(atatp)]^{2+}$ (atatp = acenaphtheno (1,2-b)-1,4,8,9-tetraazatriphenylene; L = phen (1,10-phenanthroline), bpy (2,2'-bipyridine), dmp (2,9-dimethyl-1,10-phenanthroline) and tfp (2,9-trifluoromethyl-1,10-phenanthroline) has been investigated, using the density functional theory (DFT) at the B3LYP/LanL2DZ level. The electron-structural characteristics and the trend in the DNA-binding constants (K_b) of these complexes were revealed. Based on the theoretical results, a new Ru(II) complex $[Ru(tfp)_2(atatp)]^{2+}$ (tfp =2,9-trifluoromethyl-1,10-phenanthroline)] with stronger DNA-binding ability was designed. In particular, the electronic absorption spectra of these four complexes in aqueous solution were exactly simulated using the time dependent density functional theory (TDDFT) method and the effect of the ancillary ligands on the spectra was investigated. The simulated absorption spectra of these complexes in aqueous solution are in a satisfying agreement with the experimental results and experimental absorption bands were theoretically explained in detail. These results help to directing functional molecular design as well as understanding the electron-structures and related properties of this kind of Ru(II) complex.

Key Words: Ru(II) complex, Electronic structure, DNA-binding, Spectral property, Density functional theory calculation.

INTRODUCTION

The clinical utility of Ru(II) polypyridyl-type complexes binding to DNA has inspired a great interest in design and development of novel complexes that can be applied in DNA-structure probes, DNA-molecular "light switches", DNA-photocleavage reagents, anticancer drugs and so forth[1-4]. The well-known $[Ru(phen)_2(dppz)]^{2+}$ and $[Ru(bpy)_2(dppz)]^{2+}$ complexes are the most extensively investigated complexes as DNA-molecular "light switches", because such complexes can exhibit a negligible background emission in water, but exhibit an intense luminescence in the presence of double-stranded DNA[1,2]. In order to develop novel molecular "light switch" Ru(II) complexes, a series of derivatives of $[Ru(L)_2(dppz)]^{2+}$ (L) bpy, phen) as parent complexes have been synthesized through modifying the intercalative and/or ancillary ligands to improve their luminescence properties as molecular "light switches" for DNA[5-7]. Meanwhile, more structurally analogous Ru(II) polypyridyl complexes with different shape and electronic properties have also been synthesized and their DNA-interaction properties were explored[8-15]. In addition to experimental work, many theoretical researchers have tried to correlate the experimental findings with theoretical predictions. Some studies on trends in DNA-binding affinities of this kind of Ru(II) complex applying the density functional theory (DFT) method have been reported[16-18]. However, most of them mainly focus on the effects of substituent of intercalative ligand[16-18], including our recent report on the trend in DNA-binding affinities of complexes $[Ru(bpy)_2(p\text{-R-pip})]^{2+}$ (R = -OH, $-CH_3$, -H, $-NO_2$) and $[Ru(phen)_2(L)]^{2+}$ (L = dppz, taptp, phehat)[19,20], whereas the DFT studies on the effects of ancillary ligands remain quite infrequent. Since the octahedral polypyridyl Ru(II) complexes bind to DNA in three dimensions, the ancillary ligands can play an important role in governing DNA-binding and spectral properties of these complexes. So the theoretical studies on the effects of ancillary ligands on DNA-binding and spectral properties of Ru(II) polypyridyl complexes are still very significant works for directing the functional molecular design and synthesis of transi-tion metal complexes as well as the action mechanism analysis.

In this paper, the Ru(II) polypyridyl complexes $[Ru(L)_2(atatp)]^{2+}$ atatp = acenaphtheno (1,2-b)-1,4,8,9-

tetraazatriphenylene; L = phen (1,10-phenanthroline), bpy (2,2'-bipyridine), dmp (2,9-dimethyl-1,10-phenanthroline) and tfp (2,9-trifluoromethyl-1,10-phenanthroline)[21] were selected to perform the study using the DFT method. The effects of the ancillary ligands on the electronic structures and DNA-binding properties of these complexes were revealed. Based on the theoretical results, a new Ru(II) complex $[Ru(tfp)_2(atatp)]^{2+}$ (tfp = 2,9-trifluoromethyl-1,10-phenanthroline)] with stronger DNA-binding ability was designed. In particular, the electronic absorption spectra of these four complexes in aqueous solution were exactly simulated using the time dependent density functional theory (TDDFT) method[22,23] and the effect of the ancillary ligands on the spectra was investigated. It is hoped that these theoretical efforts will help to the functional molecular design and the related property-analysis of this kind of Ru(II) complex.

COMPUTATIONAL METHODS

The studied complexes **1-4** are shown in Fig. 1. From Fig. 1, we can see that each of the complexes $[Ru(L)_2(atatp)]^{2+}$ (L = phen, bpy, dmp, tfp) forms from Ru(II) ion, one main ligand (or called as intercalative ligand) (atatp) and two co-ligands (L). Full geometry optimization of the complexes in ground state (S_0) was carried out using the restricted DFT-B3LYP method and LanL2DZ basis set[24,25]. For the obtained structures, the frequency calculations adopting the same method were also performed in order to verify the optimized structure to be an energy minimum. On the basis of the DFT optimized ground geometry, the electronic absorption spectra in aqueous solution were calculated with the time-dependent theory (TDDFT) at the level of B3LYP/LanL2DZ. 200 singlet-excited-state energies of these complexes were calculated to reproduce electronic absorption spectra. The conductor polarizable continuum model (CPCM)[26,27] was applied to the solvent effect in aqueous solution. All the calculations were preformed by means of the Gaussian03 program-package (revision D.01)[28].

RESULTS AND DISCUSSION

Ancillary ligand effect on the selected bond lengths and bond angles of the complexes: The calculated geometrical parameters of complexes **1-4** were selectively listed in Table-1. For comparison, the corresponding X-ray data of the analogs $[Ru(phen)_3][PF_6]_2$[29] were also given in Table-1.

Since the reports on the crystal structures of the four complexes have not been determined yet, the direct comparison between the computational results and the corresponding experimental data can not be performed. However, according to the comparison between the calculated results and experimental data of the analogs $[Ru(phen)_3][PF_6]_2$, we can find that the computed mean bond lengths (Ru-N_m and Ru-N_{co}) are 0.2107 nm *in vacuo* by the DFT method, which are slightly longer than the corresponding experimental mean value (0.2067 nm). The deviation of the geometric parameters optimized *in vacuo* by the DFT method from the corresponding experimental data of $[Ru(phen)_3][PF_6]_2$ is *ca.* 1.9 % for mean coordination bond length. Such a result shows that the optimized geometric

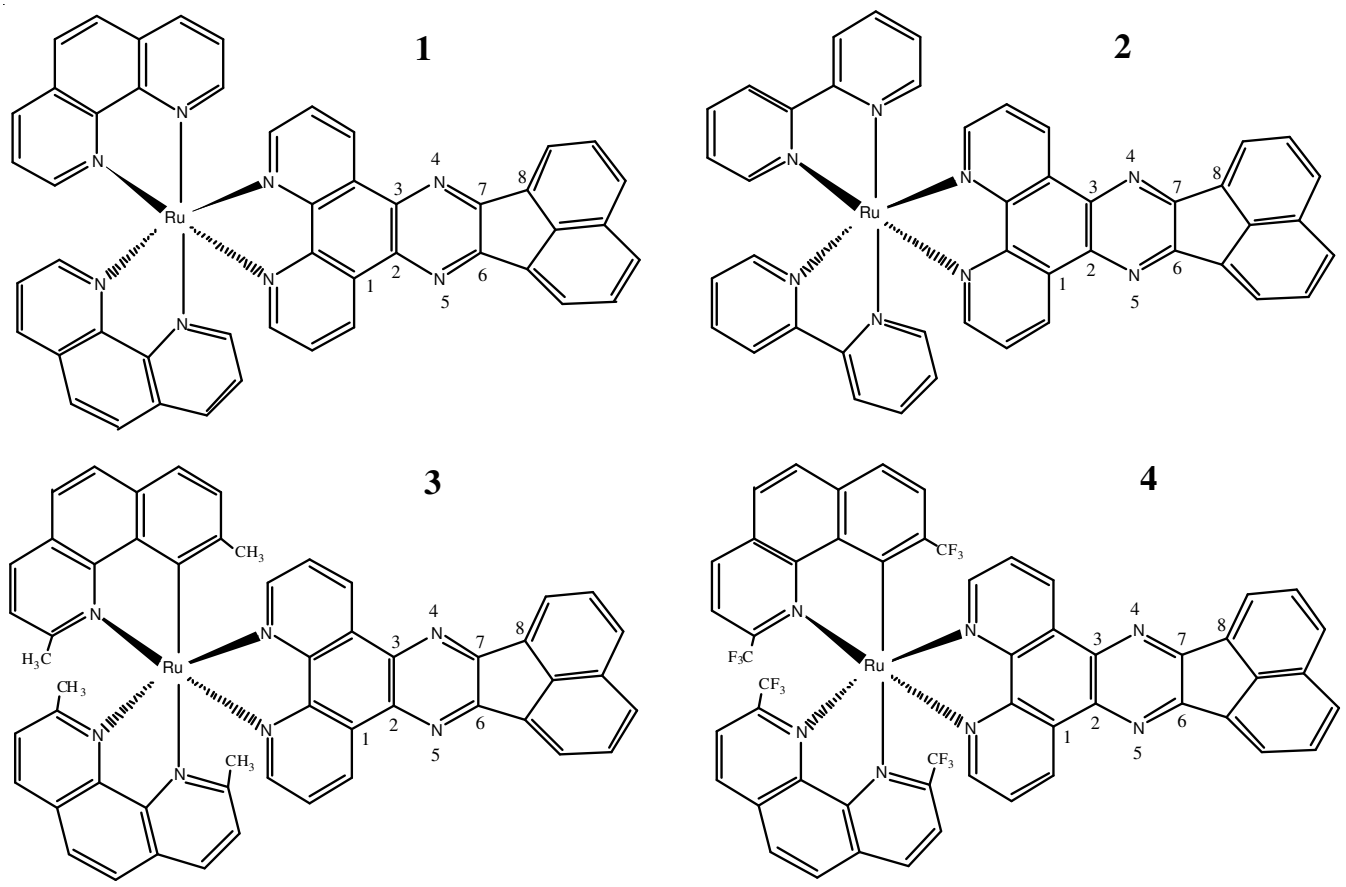

Fig. 1. Structural diagrams of the complexes **1-4** and atomic labels

TABLE-1
SELECTED COMPUTATIONAL BOND LENGTHS (nm), BOND ANGLES (º) AND DIHEDRAL ANGLES (º) OF THE COMPLEXES *in vacuo* AT THE B3LYP/LanL2DZ LEVEL

Comp.	Ru-N_m [1]	Ru-N_{co} [1]	C-C$(N)_m$ [2]	C-C$(N)_{co}$ [2]	θ_m [3]	θ_{co} [3]	β	φ
$[Ru(phen)_3]^{2+}$	0.2107	0.2107	0.1405	0.1405	79.41	79.41		
Expt [29]	0.2067	0.2067			79.9	79.9		
1 (L = phen)	0.2106	0.2106	0.1410	0.1405	79.39	79.46	–179.85	–179.95
2 (L = bpy)	0.2111	0.2096	0.1410	0.1400	79.18	78.46	–179.82	–179.91
3 (L = dmp)	0.2128	0.2156	0.1410	0.1418	78.51	79.00	–179.52	–179.83
4 (L = tfp)	0.2148	0.2158	0.4110	0.1405	77.82	79.71	–179.35	179.97

[1]Ru-N_m is the average coordination bond length between the central atom and the main ligand (atatp) and Ru-N_{co} is that between the central atom and the co-ligand (L). [2]C-C$(N)_m$ is the mean bond length of skeleton of the main ligand and C-C$(N)_{co}$ is that of the co-ligands. [3]θ_m is the coordination bond angle of the central atom and the two N atoms of the main ligand and θ_{co} is that of the central atom and the two N atoms of the co-ligands, β and φ are the dihedral angles C_1-C_2-C_3-N_4 and N_5-C_6-C_7-C_8, respectively.

structure of this kind of complex with the DFT method is substantially receivable.

From computational geometric parameters in Table-1, we can see the following: first, the coordination bond length (Ru-N_m) of the main ligand and that (Ru-N_{co}) of the co-ligands for each of complexes **1-4** are within the range of 0.2106-0.2148 nm and 0.2106-0.2158 nm, respectively. Compared among complexes **1-4**, the Ru-N_m and Ru-N_{co} of complex **4** are respectively the longest and those of complex **3** follow and those of complexes **1** and **2** are relatively shorter. Such a fact shows the following: first, introducing a methyl or a trifluoromethyl (-CF_3) group (complexes **3** and **4**) on the ancillary ligand phen (complex **1**), has a considerable effect on the Ru-N_m and Ru-N_{co}. Second, the important dihedral angles β and φ (Table-1) of these complexes are close to ± 180.0º. This indicates that the planarities of the main-ligands of complexes **1-4** are all excellent and thus the steric hindrances of their main-ligands intercalating between DNA-base-pairs should be very small.

Theoretical explanation of the trend in DNA-binding affinities of the complexes: The intrinsic binding constants K_b of the complexes **1-3** to calf thymus (CT) DNA, which quantitatively express their DNA-binding affinities, have been experimentally measured. The results show that the trend in DNA-binding constants (K_b) of the complexes **1-3** is K_b(**3**) < K_b(**2**, 7.6×10^4 M^{-1}) < K_b(**1**, 8.8×10^4 M^{-1})[21]. Such a trend can be reasonably explained by the DFT calculations.

It is well accepted that there are π-π stacking interactions between the complex and DNA-base-pairs while the complex binds to DNA in an intercalation (or part intercalation) mode[30,31]. Moreover, many theoretical studies have shown the following points: (1) The DNA base-pairs are electron donors and an intercalated complex is an electron acceptor. (2) The energies of HOMO and HOMO-x (x: small integer) of DNA-base-pairs are rather high and their components are predominately distributed on DNA-base-pairs[32]. (3) The energies of LUMO and LUMO+x of the intercalated complex are all negative and rather low and even quite lower than those of HOMO-x of DNA-base-pairs and their components are generally distributed on the main ligand of the complex. Since the DNA base-pairs as electron-donor are unchanged in present study, from the above analysis, we can see that the factors affecting DNA-binding affinities of the complexes should be the planarity, the energy and population of the lowest unoccupied molecular orbital (LUMO, even and LUMO+x) of the intercalated molecules[33,34]. The above-mentioned trend in DNA-binding affinities, *i.e.*, K_b(**3**) < K_b(**2**) < K_b(**1**), can be explained as follows: first, the energies of the LUMO+x (x = 0-2) of these complexes are all negative and rather low (Table-2) and thus it suggests these complexes are excellent electron acceptors in their DNA-binding. Second, the LUMO energies (ε_{LUMO}) follow the sequence of ε_{LUMO} (**3**, -0.2593 a.u.) > ε_{LUMO} (**1**, -0.2654 a.u.) > ε_{LUMO} (**2**, -0.2714 a.u.) > ε_{LUMO} (**4**, -0.2923 a.u.). Third, from Fig. 2, we can see that there are always some LUMO+x on which the π-components of intercalative ligands are predominantly populated. Fourth, the steric hindrances of their main-ligands intercalating between DNA-base-pairs are very small, since the planarities of the main-ligands of complexes **1-4** are all rather fine. A lower LUMO energy of complex is advantageous to accepting the electrons from DNA base pairs in an intercalative mode, because electrons or "electron-cloud" can transfer from HOMO of DNA-base-pairs to LUMO *via* inter-overlapping orbitals. So we can predict that the trend in DNA-binding constants (K_b) of these complexes is K_b(**4**) > K_b(**2**) > K_b(**1**) > K_b(**3**) *via* the analysis in LUMO energies. But such a trend is not in full agreement with the experimental results, *i.e.*, K_b(**1**) > K_b(**2**) > K_b(**3**). The reason of K_b(**1**) > K_b(**2**) can owe to the ancillary ligand phen of complex **1** possessing greater planar area than the ancillary ligand bpy of complex **2**, resulting in the hydrophobicity of complex **1** greater than that of complex **2**. So complex **1** can insert more deeply into the DNA base pairs than complex **2**, resulting in the DNA-binding constant of complex **1** to increase appreciably. Therefore, synthetically considering both energy and hydrophobicity factors, the trend in DNA-binding affinities, *i.e.*, K_b(**1**) > K_b(**2**) > K_b(**3**), can be reasonably explained. Such a theoretical result is also in agreement with the previous report[21]. Moreover, we can predict that the value of DNA-binding constant of designed complex **4** should be the greatest in complexes **1-4** because its energy of LUMO is the lowest but the conjugative area of its ancillary ligand is similar to that of complex **1**.

In summary, from the above analysis, we can see that the ancillary ligand possessing of a larger conjugated structure is advantageous to improving the DNA-binding affinity of the complex. Meanwhile, introducing a stronger electron-withdrawing trifluoromethyl (-CF_3) on the ancillary ligands is advantageous to reducing the energies of LUMO+x and thus to increasing the DNA-binding constant of the complex, whereas introducing a stronger electron-donating methyl

TABLE-2
SOME FRONTIER MOLECULAR ORBITAL ENERGIES (a.u.) OF THE COMPLEXES **1-4** *in vacuo* AT THE B3LYP/LanL2DZ LEVEL

Compd.	HOMO-2	HOMO-1	HOMO	LUMO	LUMO+1	LUMO+2
1	–0.3906	–0.3859	–0.3685	–0.2654	–0.2621	–0.2589
2	–0.3938	–0.3879	–0.3701	–0.2714	–0.2682	–0.2595
3	–0.3847	–0.3838	–0.3690	–0.2593	–0.2592	–0.2544
4	–0.3944	–0.3880	–0.3696	–0.2923	–0.2901	–0.2870

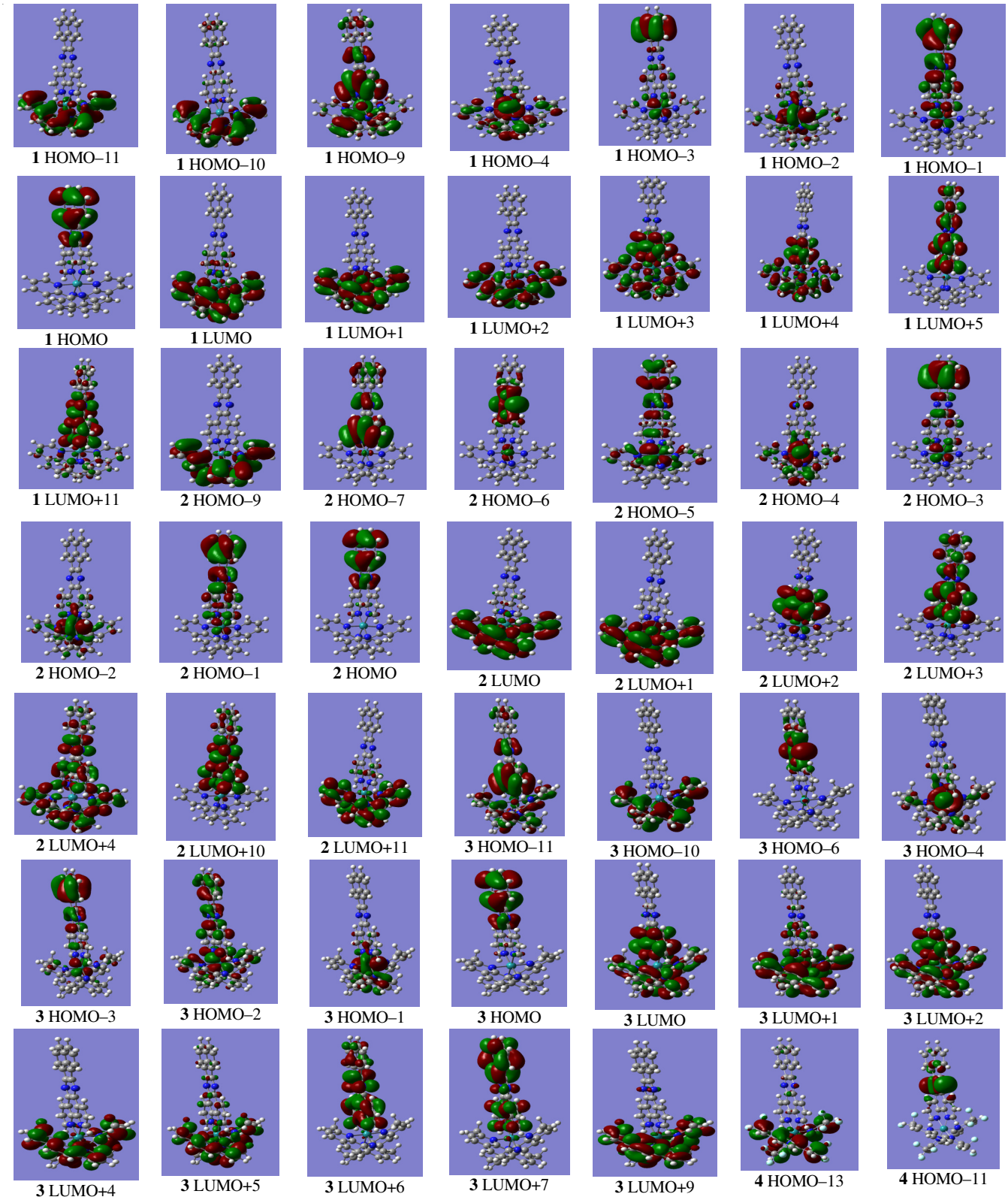

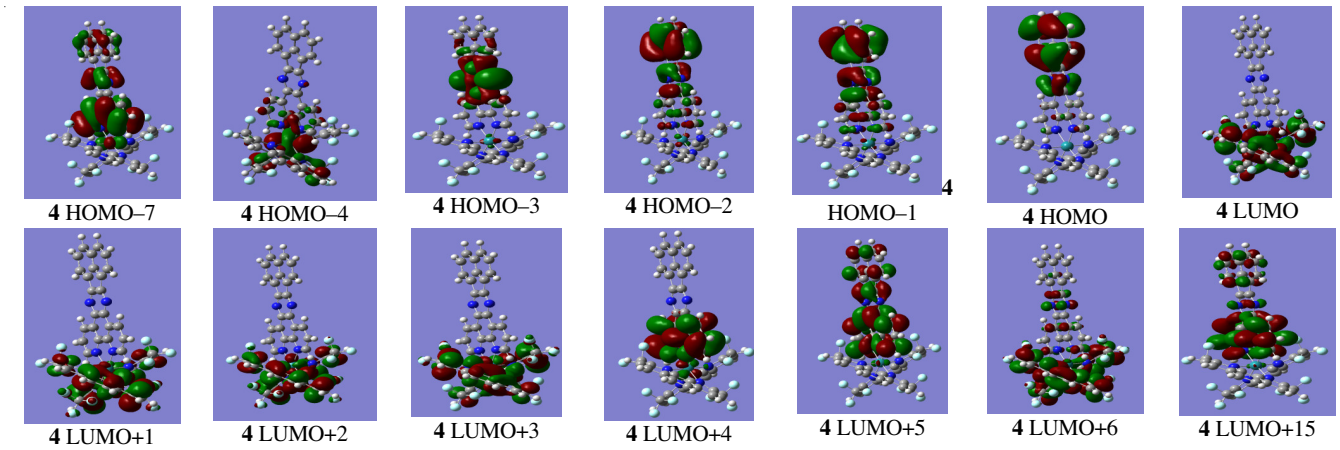

Fig. 2. Contour plots of three high occupied and three low unoccupied molecular orbitals as well as some related frontier molecular orbitals of complexes **1-4** using the DFT method at the B3LYP/LanL2DZ level

(-CH_3) on the ancillary ligands is disadvantageous to increasing the DNA-binding constant of the complex.

Theoretical explanation on the spectral properties: The calculated absorption spectra of all the four complexes with the TDDFT method and the corresponding experimental absorption spectra are given in Fig. 3. In order to explain the experimental absorption bands, the calculated excitation energies (ΔE/eV) oscillator strengths ($f \geq 0.20$), main orbital transition contributions (≥ 25 %) as well as the experimental values are given in Table-3. Meanwhile, a few states with very low oscillator strengths (between 0.1-0.2) are also indicated when necessary for the discussion.

From Table-3, we can find the following:

For complex **1**, the band at 448.5 nm mainly involves the transitions of HOMO-2→LUMO+1 and HOMO-2→LUMO+2 and it can be characterized by $d_{Ru}\rightarrow\pi^*_{co}$, with an obvious metal-to-ligand charge transfer character. The band at 435.5 nm mainly involves the transitions of HOMO-1→LUMO+4 and HOMO-1→LUMO and it can be characterized by $d_{Ru}\rightarrow\pi^*_{co}$ and $\pi_m\rightarrow\pi^*_{co}$, with obvious metal-to-complex and ligand-to-ligand charge transfer characters. The band at 374.5 nm mainly involves the transitions of HOMO-3→LUMO and it can be characterized by $d_{Ru}\rightarrow\pi^*_{co}$ and $\pi_m\rightarrow\pi^*_{co}$, with obvious metal-to-ligand and ligand-to-ligand

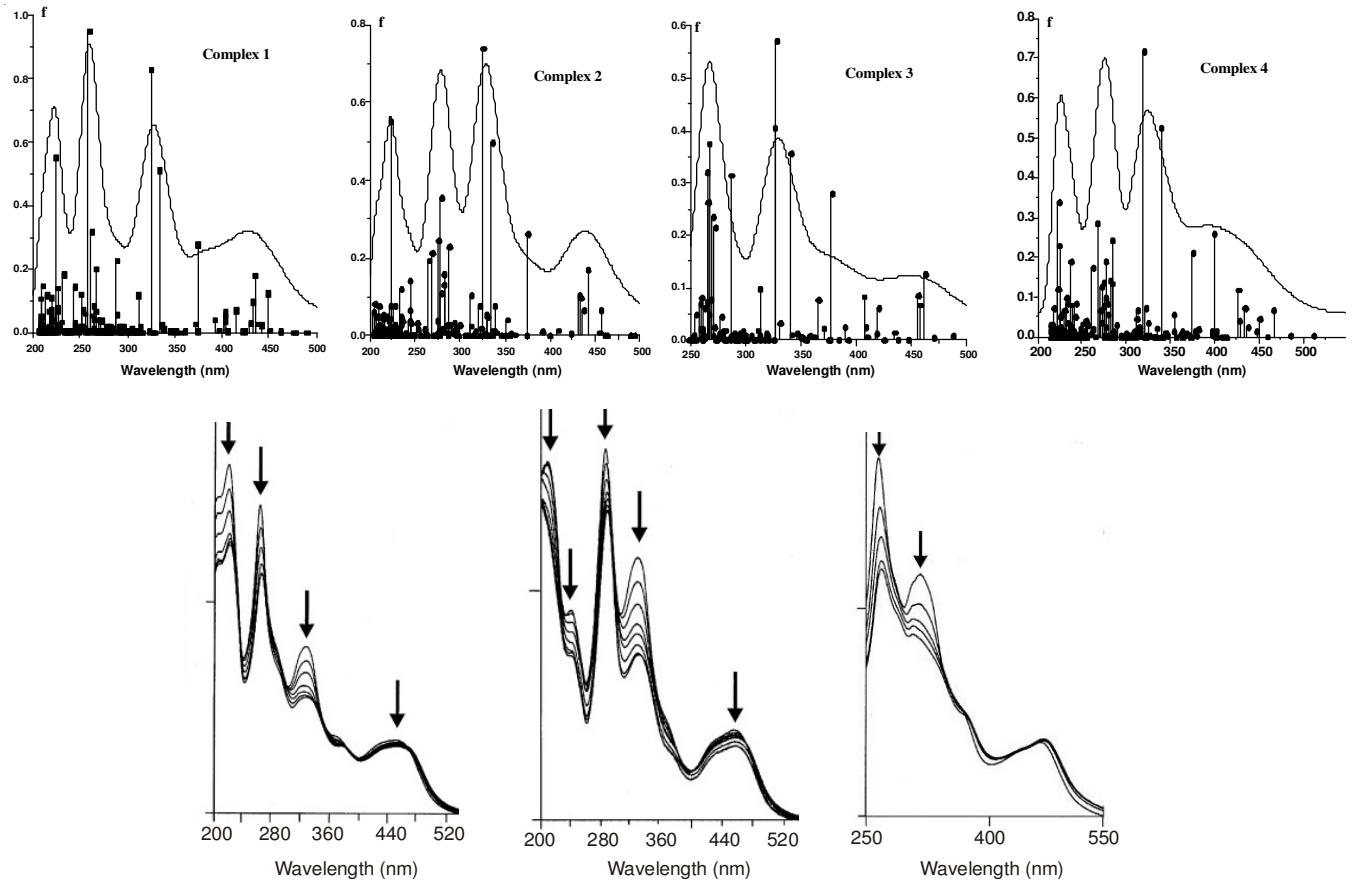

Fig. 3. Calculated absorption spectra of complexes **1-4** in aqueous solution and corresponding experimental ones (the bottom) [Ref. 21]

TABLE-3
CALCULATED EXCITATION ENERGIES (ΔE/eV), OSCILLATOR STRENGTHS AND MAIN ORBITAL TRANSITION CONTRIBUTIONS OF COMPLEXES **1**-**4** IN AQUEOUS SOLUTION AS WELL AS THE EXPERIMENTAL VALUES[21]

No	Major contribution	ΔE (eV)	*f*	λ/nm (calc.)	λ/nm (simu.)	λ/nm (expt.)	Character
1	H-2→L+1	2.76	0.124	448.5			$d_{Ru}\rightarrow\pi^*_{co}$
	H-2→L+2						$d_{Ru}\rightarrow\pi^*_{co}$
	H-1→L+4	2.85	0.181	435.5	434.0	447.0	$d_{Ru}\rightarrow\pi^*_{co}$ and $\pi_m\rightarrow\pi^*_{co}$
	H-1→L						$d_{Ru}\rightarrow\pi^*_{co}$ and $\pi_m\rightarrow\pi^*_{co}$
	H-3→L	3.31	0.278	374.5			$d_{Ru}\rightarrow\pi^*_{co}$ and $\pi_m\rightarrow\pi^*_{co}$
	H-4→L+1	3.71	0.513	334.4			$d_{Ru}\rightarrow\pi^*_{co}$
	H-4→L+2	3.81	0.830	325.0	327.0	326.0	$d_{Ru}\rightarrow\pi^*_{co}$
	H-4→L+3						$d_{Ru}\rightarrow\pi^*_{co}+\pi^*_m$
	H-10→L	4.30	0.230	288.5			$\pi_{co}\rightarrow\pi^*_{co}$
	H-9→L+5	4.65	0.202	266.7			$d_{Ru}\rightarrow\pi^*_m$ and $\pi_{co}\rightarrow\pi^*_m$
	H-11→L+4	4.76	0.318	260.7			$\pi_{co}\rightarrow\pi^*_m$
	H-9→L+4	4.80	0.949	258.5	259.0	268.6	$d_{Ru}\rightarrow\pi^*_{co}$ and $\pi_m\rightarrow\pi^*_{co}$
	H-3→L+11	5.55	0.553	223.5	223.0	222.9	$d_{Ru}\rightarrow\pi^*_m$ and $\pi_m\rightarrow\pi^*_m$
2	H-2→L	2.80	0.169	442.2	440.0	451.0	$d_{Ru}\rightarrow\pi^*_{co}$
	H-2→L+3						$d_{Ru}\rightarrow\pi^*_m$
	H-2→L+2	2.86	0.100	433.4			$d_{Ru}\rightarrow\pi^*_m$
	H-1→L+3						$d_{Ru}\rightarrow\pi^*_m$
	H-2→L	2.87	0.106	431.8			$d_{Ru}\rightarrow\pi^*_{co}$
	H-3→L	3.31	0.265	374.8			$d_{Ru}\rightarrow\pi^*_{co}$ and $\pi_m\rightarrow\pi^*_{co}$
	H-4→L+1	3.70	0.499	335.6			$d_{Ru}\rightarrow\pi^*_{co}$
	H-4→L+2	3.81	0.741	325.0	328.0	327.0	$d_{Ru}\rightarrow\pi^*_m$, $\pi_{co}\rightarrow\pi^*_m$
	H-4→L+4						$d_{Ru}\rightarrow\pi^*_{co}$ and $d_{Ru}\rightarrow\pi^*_m$
	H-9→L	4.31	0.229	287.9			$\pi_{co}\rightarrow\pi^*_{co}$
	H-7→L+3	4.45	0.357	278.9	279.0	285.7	$\pi_m\rightarrow\pi^*_m$
	H-6→L+4	4.49	0.247	275.9			$\pi_m+d_{Ru}\rightarrow\pi^*_m+\pi^*_{co}$
	H-5→L+4	4.61	0.212	269.2			$d_{Ru}\rightarrow\pi^*_{co}$
	H-2→L+10						$d_{Ru}\rightarrow\pi^*_m$
	H-3→L+11	5.55	0.552	223.6	224.0	211.4	$d_{Ru}\rightarrow\pi^*_{co}$, $\pi^*_m\rightarrow\pi^*_{co}$
3	H-1→L+1	2.68	0.126	462.2	459.0	463.0	$d_{Ru}\rightarrow\pi^*_m+\pi^*_{co}$
	H-3→L	3.28	0.280	377.8			$d_{Ru}+\pi_m\rightarrow\pi^*_{co}+\pi^*_m$
	H-4→L+1	3.64	0.356	341.0			$d_{Ru}\rightarrow\pi^*_m+\pi^*_{co}$
	H-4→L+2	3.78	0.574	328.0	330.0	325.0	$d_{Ru}\rightarrow\pi^*_m+\pi^*_{co}$
	H-2→L+7						$d_{Ru}\rightarrow\pi^*_m$, $\pi_{co}\rightarrow\pi^*_m$
	H-4→L+2	3.80	0.407	326.4			$d_{Ru}\rightarrow\pi^*_m+\pi^*_{co}$
	H-2→L+7						$d_{Ru}\rightarrow\pi^*_m$, $\pi_{co}\rightarrow\pi^*_m$
	H-11→L	4.32	0.315	287.1			$\pi_m\rightarrow\pi^*_{co}$
	H-2→L+9	4.56	0.217	272.1			$d_{Ru}+\pi_m\rightarrow\pi^*_{co}$
	H-6→L+6	4.58	0.237	270.6			$\pi_m\rightarrow\pi^*_m$
	H-10→L+5	4.64	0.376	267.2	267.0	267.6	$\pi_{co}\rightarrow\pi^*_{co}$
	H-11→L+4	4.66	0.266	265.9			$\pi_m\rightarrow\pi^*_{co}$
	H-10→L+5						$\pi_{co}\rightarrow\pi^*_{co}$
	H-11→L+4	4.67	0.320	265.3			$\pi_m\rightarrow\pi^*_{co}$
4	H-4→L+2	3.11	0.261	399.2	400.0		$d_{Ru}\rightarrow\pi^*_{co}$
	H-2→L+3						$\pi_m\rightarrow\pi^*_{co}$, $\pi_m\rightarrow d^*_{Ru}$
	H→L+4	3.31	0.213	374.5			$\pi_m\rightarrow\pi^*_m$
	H-2→L+6	3.65	0.528	339.7			$\pi_m\rightarrow\pi^*_{co}$
	H-3→L+6	3.88	0.717	319.2	323.0		$\pi_m\rightarrow\pi^*_{co}$
	H-7→L+4	4.36	0.245	284.6			$\pi_m\rightarrow\pi^*_m$
	H-11→L+3	4.63	0.285	267.7	270.0		$\pi_m\rightarrow\pi^*_{co}$, $\pi_m\rightarrow d^*_{Ru}$
	H-13→L+5	5.53	0.231	224.2			$\pi_{co}\rightarrow\pi^*_m$
	H→L+15	5.55	0.339	223.6	225.0		$\pi_m\rightarrow\pi^*_m$

charge transfer characters. The simulated absorption band at about 434 nm can be assigned to a superposition of the above three strong bands and it is in a satisfying agreement with the experimental absorption band at 447 nm. The band at 334.4 nm mainly involves the transitions of HOMO-4→LUMO+1 and it can be characterized by $d_{Ru}\rightarrow\pi^*_{co}$, with an obvious metal-to-ligand charge transfer character. The band at 325 nm mainly involves the transitions of HOMO-4→LUMO+2 and HOMO-4→LUMO+3, it can be characterized by $d_{Ru}\rightarrow\pi^*_{co}$ and $d_{Ru}\rightarrow\pi^*_{co}+\pi^*_m$, with an obvious metal-to-ligand charge transfer character. The simulated absorption band at about 327 nm can be assigned to a superposition of the above three strong bands and it is in a satisfying agreement with the experimental absorption band at 326 nm. In addition, the other simulated absorption bands at about 259 nm and 223 nm, with obvious metal-to-ligand and ligand-to-ligand charge transfer characters,

are in a satisfying agreement with the experimental absorption band observed at 268.6 nm and 222.9 nm, respectively.

For complex **2**, the band at 442.2 nm mainly involves the transitions of HOMO-2→LUMO and HOMO-2→LUMO+3 and it can be characterized by $d_{Ru}\rightarrow\pi^*_{co}$ and $d_{Ru}\rightarrow\pi^*_{m}$, respectively, with an obvious metal-to-ligand charge transfer character. The band at 433.4 nm mainly involves the transitions of HOMO-2→LUMO+2 and HOMO-1→LUMO+3 and it can be characterized by $d_{Ru}\rightarrow\pi^*_{m}$, with an obvious metal-to-complex charge transfer character. The band at 431.8 nm mainly involves the transition of HOMO-2→LUMO and it can be characterized by $d_{Ru}\rightarrow\pi^*_{co}$, with an obvious metal-to-complex charge transfer character. The simulated absorption band at about 440 nm can be assigned to a superposition of the above three strong bands and it is in a satisfying agreement with the experimental absorption band at 451 nm. The band at 335.6 nm mainly involves the transition of HOMO-4→LUMO+1 and it can be characterized by $d_{Ru}\rightarrow\pi^*_{co}$, with an obvious metal-to-ligand charge transfer character. The band at 325 nm mainly involves the transitions of HOMO-4→LUMO+2 and HOMO-4→LUMO+4 and it can be characterized by $d_{Ru}\rightarrow\pi^*_{m}$, $\pi_{co}\rightarrow\pi^*_{m}$ and $d_{Ru}\rightarrow\pi^*_{co}$, with an obvious metal-to-ligand and ligand-to-ligand charge transfer characters. The simulated absorption band at about 328 nm can be assigned to a superposition of the above two strong bands and it is in a satisfying agreement with the experimental absorption band at 327 nm. In addition, the other simulated absorption bands at about 279 nm and 224 nm, with obvious metal-to-ligand and ligand-to-ligand charge transfer characters, are in a satisfying agreement with the experimental absorption band observed at 285.7 nm and 211.4 nm, respectively.

For complex **3**, ten strong transitions with $f > 0.2$, lie in the range of 250-500 nm. Both bands at 328 nm ($f = 0.574$) and 326.4 nm ($f = 0.407$), mainly involve the transitions from HOMO-4→LUMO+2 and HOMO-2→LUMO+7 and they mainly be characterized by $d_{Ru}\rightarrow\pi^*_{m} + \pi^*_{co}$ and $\pi_{co}\rightarrow\pi^*_{m}$, with obvious metal-to-ligand and ligand-to-ligand charge transfer characters. The band at 341 nm ($f = 0.356$), mainly involves the transition from HOMO-4→LUMO+1 and it mainly be characterized by $d_{Ru}\rightarrow\pi^*_{m} + \pi^*_{co}$, with an obvious metal-to-ligand charge transfer character. The simulated absorption band at about 330 nm can be assigned to a superposition of the above three strong bands and it is in a satisfying agreement with the experimental absorption band at 325 nm. The band at 462.2 nm, mainly involves the transition from HOMO-1→LUMO+1 and it mainly be characterized by $d_{Ru}\rightarrow\pi^*_{m} + \pi^*_{co}$. The simulated absorption band at about 458 nm is mainly made up of the above band, which is in a satisfying agreement with the experimental absorption band at 463 nm. In addition, six high-energy bands at 287.1, 272.1, 270.6, 267.2, 265.9 and 265.3 nm are mainly attributed to the $\pi_m + \pi_{co}\rightarrow\pi^*_{co} + \pi^*_{m}$ and few $d_{Ru}\rightarrow\pi^*_{co}$ transitions. The simulated absorption band at about 267 nm can be assigned to a superposition of the above six strong bands and it is in a satisfying agreement with the experimental absorption band observed at about 267.6 nm.

For complex **4**, there are four simulated absorption bands observed at 400, 323, 270 and 225 nm. The band at 400 nm can be assigned to a superposition of two bands (399.2 and 374.5 nm) with metal-to-ligand, ligand-to-ligand and ligand-to-metal charge transfer characters. The band at 323.0 nm can be assigned to a superposition of two bands (339.7 and 319.2 nm) with an obvious ligand-to-ligand charge transfer character. The band at 270 nm can be assigned to a superposition of two bands (284.6 and 267.7 nm) with ligand-to-ligand and ligand-to-metal charge transfer characters. The band at 225 nm can be assigned to a superposition of two bands (224.2 and 223.6 nm) with an obvious ligand-to-ligand charge transfer character. These calculated spectra of complex **4** are waiting for experimental confirmation.

In summary, the absorption spectra of the four complexes can be simulated and discussed minutely by the TDDFT computations. For complexes **1-3**, the low-energy bands are mainly attributed to the transitions of d→π*, with an obvious metal-to-ligand charge transfer character. Compared complex **4** with complex **1**, we can see that the substitution of an electron-withdrawing $-CF_3$ for H on the ancillary ligands can change the electron transition feature, *i.e.*, mainly from d→π* to π→π* and make the maximum absorption band blue-shift. The increase in the conjugated planar area of the ancillary ligand can also make the maximum absorption band blue-shift (see complexes **1** and **2**). Compared complex **3** with complex **1**, we can see that the substitution of a stronger electron donating $-CH_3$ for H on the ancillary ligands can make the maximum absorption band red-shift. In particular, the spectra of designed complex **4** with greater DNA-binding ability has been simulated, predicted and explained.

Conclusion

The DFT studies of a series of complexes $[Ru(L)_2(atatp)]^{2+}$ (L = phen, bpy, dmp) **1-3** show that modification of ancillary ligand has important effect on the electronic structures, trend in the DNA-binding affinities and spectral properties of these complexes. Based on these results, a new R(II) complex $Ru(tfp)_2(atatp)]^{2+}$ **4** with greater DNA-binding ability was designed. In summary, some conclusions can be drawn as follows: (1) the ancillary ligand possessing a conjugated structure and a great planar area can improve the DNA-binding affinity of the complex. (2) Introducing a stronger electron-donating group ($-CH_3$) on the ancillary ligand is disadvantageous to increasing the DNA-binding constant (K_b) of the complex, whereas introducing a stronger electron-donating group ($-CF_3$) is in contrary. Therefore, the designed complex **4** can be expected to have the greatest K_b value in complexes **1-4**. (3) The increase in the conjugated planar area of the ancillary ligand can make the maximum absorption band blue-shift. (4) The substitution of an electron-withdrawing $-CF_3$ for H on the ancillary ligands can change the electron transition feature, *i.e.*, mainly from d→π* to π→π* and can also make the maximum absorption band blue-shift, whereas the substitution of a stronger electron-donating $-CH_3$ for H on the ancillary ligands can make the maximum absorption band red-shift. In addition, the electronic absorption spectra of these complexes in aqueous solution were exactly simulated and explained using the DFT/TDDFT methods, in a satisfying agreement with the experimental results.

ACKNOWLEDGEMENTS

The authors are pleased to thank the financial support of the National Natural Science Foundation of China (20903025). Meanwhile, we heartily thank the Information & Network Center, Sun Yat-Sen University for offering the High Performance Computing Clusters (HPCC).

REFERENCES

1. R.M. Hartshorn and J.K. Barton, *J. Am. Chem. Soc.*, **114**, 5919 (1992).
2. A.E. Friedman, J.C. Chambron, J.P. Sauvage, N.J. Turro and J.K. Barton, *J. Am. Chem. Soc.*, **112**, 4960 (1990).
3. L.N. Ji, X.H. Zou and J.G. Liu, *Coord. Chem. Rev.*, **216-217**, 513 (2001).
4. P. Nordell and P. Lincoln, *J. Am. Chem. Soc.*, **127**, 9670 (2005).
5. S. Arounaguiri and B.G. Maiya, *Inorg. Chem.*, **38**, 842 (1999).
6. K.A. O'Donoghue, J.M. Kelly and P.E. Kruger, *J. Chem. Soc., Dalton. Trans.*, 13 (2004).
7. Q.X. Zhen, B.H. Ye, J.G. Liu, Q.L. Zhang, L.N. Ji and L. Wang, *Inorg. Chim. Acta*, **303**, 141 (2000).
8. W.J Mei, Y.J. Liu, N. Wang, Y.Z. Ma, H. Wang, L.Q. Luo and S.L. Huang, *Transition Met. Chem.*, **31**, 1024 (2006).
9. P.K.L. Fu, P.M. Bradley, D. van Loyen, H. Durr, S.H. Bossmann and C. Turro, *Inorg. Chem.*, **41**, 3808 (2002).
10. X.W. Liu, J. Li, H. Li, K.C. Zheng, H. Chao and L.N. Ji, *J. Inorg. Biochem.*, **99**, 2372 (2005).
11. L.F. Tan, H. Chao, H. Li, Y.J. Liu, B. Sun, W. Wei and L.N. Ji, *J. Inorg. Biochem.*, **99**, 513 (2005).
12. B. Elias and A. Kirsch-De Mesmaeker, *Coord. Chem. Rev.*, **250**, 1627 (2006).
13. B. Elias, J.M. Kelly, C. Creely, G.W. Doorley, M.M. Feeney, C. Moucheron, A. Kirsch-DeMesmaeker, J. Dyer, D.C. Grills, M.W. George, P. Matousek, A.W. Parker and M. Towrie, *Chem. Eur. J.*, **14**, 369 (2008).
14. H. Uji-i, P. Foubert, F.C. De Schryver, S. De Feyter, E. Gicquel, A. Etoc, C. Moucheron and A. Kirsch-De Mesmaeker, *Chem. Eur. J.*, **12**, 758 (2006).
15. I. Ortmans, B. Elias, J.M. Kelly, C. Moucheron and A. Kirsch-DeMesmaker, *J. Chem. Soc. Dalton Trans.*, 668 (2004).
16. K.C. Zheng, J.P. Wang, W.L. Peng, X.W. Liu and F.C.Yun, *J. Phys. Chem. A*, **105**, 10899 (2001).
17. S. Shi, M. Liu, K.C. Zheng, C.P. Tan, L.M. Chen and L.N. Ji, *J. Chem. Soc. Dalton Trans.*, 2038 (2005).
18. X.W. Liu, J. Li, H. Deng, K.C. Zheng, Z.W. Mao and L.N. Ji, *Inorg. Chim. Acta*, **358**, 3311 (2005).
19. J. Li, L.C. Xu, J.C. Chen, K.C. Zheng and L.N. Ji, *J. Phys. Chem. A*, **110**, 8174 (2006).
20. J. Li, J.C. Chen, L.C. Xu, K.C. Zheng and L.N. Ji, *J. Organomet. Chem.*, **692**, 831 (2007).
21. Q.X. Zhen, Q.L. Zhang, J.G. Liu, B.H. Ye, L.N. Ji and L. Wang, *J. Inorg. Biochem.*, **78**, 293 (2000).
22. Q.L. Wei, S.S. Zhang, J. Gao and X.M. Li, *Asian J. Chem.*, **19**, 1461 (2007).
23. R. Kanakaraju and P. Kolandaivel, *Int. J Mol. Sci.*, **3**, 777 (2002).
24. P.J. Hay and W.R. Wadt, *J. Chem. Phys.*, **82**, 270 (1985).
25. W.R. Wadt and P.J. Hay, *J. Chem. Phys.*, **82**, 284 (1985).
26. V. Barone and M. Cossi, *J. Phys. Chem. A*, **102**, 1995 (1998).
27. M. Cossi, N. Rega, G. Scalmani and V. Barone, *J. Comp. Chem.*, **24**, 669 (2003).
28. M.J. Frisch, G.W. Trucks, H.B. Schlegel, G.E. Scuseria, M.A. Robb, J.R. Cheeseman, J.A. Montgomery Jr., T. Vreven, K.N. Kudin, J.C. Burant, J.M. Millam, S.S. Iyengar, J. Tomasi, V. Barone, B. Mennucci, M. Cossi, G. Scalmani, N. Rega, G.A. Petersson, H. Nakatsuji, M. Hada, M. Ehara, K. Toyota, R. Fukuda, J. Hasegawa, M. Ishida, T. Nakajima, Y. Honda, O. Kitao, H. Nakai, M. Klene, X. Li, J.E. Knox, H.P. Hratchian, J.B. Cross, V. Bakken, C. Adamo, J. Jaramillo, R. Gomperts, R.E. Stratmann, O. Yazyev, A.J. Austin, R. Cammi, C. Pomelli, J.W. Ochterski, P.Y. Ayala, K. Morokuma, G.A. Voth, P. Salvador, J.J. Dannenberg, V.G. Zakrzewski, S. Dapprich, A. D. Daniels, M.C. Strain, O. Farkas, D.K. Malick, A.D. Rabuck, K. Raghavachari, J.B. Foresman, J. V. Ortiz, Q. Cui, A.G. Baboul, S. Clifford, J. Cioslowski, B.B. Stefanov, G. Liu, A. Liashenko, P. Piskorz, I. Komaromi, R.L. Martin, D.J. Fox, T. Keith, M.A. Al-Laham, C.Y. Peng, A. Nanayakkara, M. Challacombe, P.M.W. Gill, B. Johnson, W. Chen, M.W. Wong, C. Gonzalez, J.A. Pople, Gaussian 03, Revision D.01; Gaussian, Inc.: Wallingford CT (2005).
29. D.J. Maloney and F.M. MacDonnell, *Acta Crystallogr.*, **53C**, 705 (1997).
30. A.M. Pyle, J.P. Rehmann, R. Meshoyrer, C.V. Kumar, N.J. Turro and J.K. Barton, *J. Am. Chem. Soc.*, **111**, 3051 (1989).
31. C. Hiort, P. Lincoln and B. Nordén, *J. Am. Chem. Soc.*, **115**, 3448 (1993).
32. D. Reha, M. Kabelác, F. Ryjácek, J. Šponer, J.E. Šponer, M. Elstner, S. Sándor and P. Hobza, *J. Am. Chem. Soc.*, **124**, 3366 (2002).
33. H. Xu, K.C. Zheng, H. Deng, L.J. Lin, Q.L. Zhang and L.N. Ji, *New J. Chem.*, **27**, 1255 (2003).
34. S. Shi, J. Liu, J. Li, K.C. Zheng, X.M. Huang, C.P. Tan, L.M. Chen and L.N. Ji, *J. Inorg. Biochem.*, **100**, 385 (2006).